Proceedings of the ASME 2025
International Design Engineering Technical Conferences and
Computers and Information in Engineering Conference
IDETC-CIE2025
August 17-20, 2025, Anaheim, CA

DETC2025-169745

ANALYTICAL EXPLORATION OF THE NONLINEAR DYNAMICS OF A HAND-ARM SYSTEM COUPLED WITH A TOOL EXHIBITING NON-SMOOTH GROUND INTERACTION

Oreoluwa Alabi, Sunit Kumar Gupta, Oumar Barry*
Department of Mechanical Engineering
Virginia Polytechnic Institute and State University
Blacksburg, Virginia 24061

ABSTRACT

This paper investigates the nonlinear vibration behavior of a chipping hammer to improve the understanding of how grazing influences the vibrations transmitted to the hand-arm system. The motivation for this work stems from the need to better characterize how vibrations to the hand are transferred from a tool. This is important particularly since severe exposure of vibrations to the hand can lead to severe health effects, including permanent disability. Predicting the nature of these vibrations offers a pathway toward developing strategies to mitigate harmful transmission to the user. To address the understanding of the transmission of vibrations to the hand, a vibroimpact model is adopted to capture the nonlinear dynamics typical of percussive tools. The model, coupled with a representation of the hand-arm system, is tuned so that its natural frequency matches experimentally observed values for a chipping hammer. Using a numerical solver and the COCO continuation toolbox, the onset and disappearance of grazing in the system is systematically identified. To the authors' knowledge, this is the first study to apply continuation methods to track grazing in a hybrid model that explicitly couples tool dynamics with a hand-arm system. These grazing events are found to vary with the excitation amplitude of the tool. Additionally, a parametric study is conducted to evaluate how changes in feed force influence grazing behavior and the resulting hand-arm acceleration. Results show that feed force significantly shifts the regions in the chipping hammer excitation force - frequency parameter space where grazing occurs. Vibration levels at the hand where also observed to alter in the different regions of the system exhibiting various levels of grazing.

INTRODUCTION

Various studies have highlighted the impact of severe vibration exposure on the hand-arm system [1, 2]. Prolonged use of hand-held tools can lead to hand-arm vibration syndrome (HAVS), a disorder characterized by vascular, musculoskeletal, and neurological complications [3–6]. One of the primary symptoms of HAVS is vibration white finger (VWF), which can progress to permanent disability in extreme cases [7–10]. To assess the risk posed by vibration exposure to the hand, this study focuses on a key contributing factor—vibration intensity, as measured by acceleration—by analyzing the nonlinear dynamics that govern the operation of a hand-held impact tool. Understanding the mechanisms through which vibrations are transmitted to the hand is the central aim of this paper. A deeper understanding of these dynamics provides a foundation for selecting appropriate vibration control strategies, thereby reducing the risk of long-term adverse health effects among hand-tool users.

Towards addressing the problem of how vibrations are propagated to the hand, various models have been proposed to accurately capture the tool-hand dynamics. These models aim to assess the transmission of vibrations from the tool to the hand and include lumped parameter linear models as well as models incor-

*Corresponding Author (Email: obarry@vt.edu)

porating cubic and piecewise nonlinearities [11–14]. Such nonlinearities are typically introduced through the dynamics of the tool itself. It has been shown that models with piecewise-smooth nonlinearities more effectively capture the physics of repetitive impacts or discontinuous contact events that occur during tool operation [15–22]. For instance, in the modeling of rotary oil drilling systems, the combined effects of cutting and frictional interactions between the bit and rock were captured using a nonsmooth model based on Stribeck friction [23]. In efforts to optimize the rate of drilling progression, Pavlovskaia *et al.* showed that nonsmooth models could best predict the static and dynamic forces that produced the most efficient vibroimpact drilling performance [16]. Similarly, to represent the nonlinear interaction between the bit and rock, Liao *et al.* compared linear and nonlinear models capturing loading and unloading force-penetration dynamics and found that both, while piecewise-smooth, could accurately model the dynamics at low excitation frequencies and small amplitudes [24]. Wiercigroch *et al.* also used a piecewise system to predict the material removal rate of an ultrasonic drill under varying static loads [25]. Given the demonstrated ability of lumped parameter models with nonsmooth or vibroimpact dynamics to capture essential features of percussive tools, this work adopts the approach of Alabi *et al.* [26] to investigate how vibrations are transmitted to the hand by modeling the tool as a vibroimpact system. To fully analyze such a system, it is critical to understand the conditions under which the system transitions between different states, and what qualitative behavior emerges during and after those transitions. In particular, we are interested in understanding how these dynamics influence the magnitude of acceleration transmitted to the hand. To this end, we examine grazing phenomena—a hallmark of nonsmooth systems with impacts such as the one considered here [27–30].

Grazing is defined as a phenomenon that occurs when a mass just makes tangential contact with an impact surface. It has been widely recognized that grazing in nonsmooth systems can induce abrupt transitions in the underlying dynamics. These transitions may include the appearance or disappearance of multistable attractors, loss of stability, onset of chaotic behavior, and emergence of vulnerable attractors [31–35]. Analyzing the post-grazing dynamics is essential, as these changes in steady-state behavior would not arise in the absence of the discontinuities that characterize nonsmooth systems. For instance, in atomic force microscopy, grazing transitions have been linked to the sudden termination of periodic solution branches due to hysteretic force interactions [36]. Moreover, metrology errors have been attributed to the transition from periodic to chaotic responses when microcantilever tips experience grazing in dynamic atomic force microscopy [37]. In the analysis of impact oscillators, grazing has been shown to cause the disappearance of stable periodic motion [38]. Similarly, in an aeroelastic system modeled as a nonsmooth dynamical system, the occurrence of grazing bifurcations was found to induce abrupt jumps in system response [39]. Given the dramatic transitions that grazing can trigger in system behavior, it is imperative to study nonsmooth systems exhibiting grazing using analysis methods that allow these events to be accurately tracked. To this end, we now turn our attention to a review of methods previously used to analyze the dynamics of nonsmooth systems.

Several techniques have been developed to analyze nonsmooth systems, including numerical integration methods and path-following continuation approaches. One of the more common strategies involves smoothing the nonsmooth differential equations, which enables the use of standard numerical tools such as numerical bifurcation analysis. In such formulations, the state space is partitioned into subspaces, each governed by a smooth ordinary differential equation [40, 41]. This technique was used by Savi *et al.* to validate experimentally observed chaos and period-doubling behavior in a nonsmooth system with a discontinuous support [42]. Similarly, smoothed approximations have been employed to study the stability of a single-degree-of-freedom system with a piecewise-linear force–displacement relationship under harmonic excitation [43]. Another powerful method for analyzing nonsmooth dynamics is path-following continuation, which allows for tracking critical behaviors such as bifurcations and limit cycles in parameter space. For example, Zhang *et al.* used the continuation toolbox COCO to compute grazing periodic orbits in a hybrid dynamical system and investigated the effectiveness of time-delayed feedback control in suppressing undesirable dynamics near grazing [44]. Chavez *et al.* also used COCO to track controller parameters that influence the occurrence of grazing in a forced impact oscillator [45]. In this work, due to the hybrid nature of the nonsmooth tool model under investigation, we begin with direct numerical integration of a smoothed set of ODEs using MATLAB's `ODE45` solver. We then employ COCO to track grazing periodic orbits that arise in the system. A novel contribution of this work lies in exploring whether grazing affects the acceleration transmitted to the hand, and in conducting a parametric study to examine how key variables—such as feed force—influence the onset of grazing in the system. While continuation techniques have been used to analyze grazing in various mechanical and control systems [44, 45], previous studies have not applied such methods to models that include both the vibroimpact dynamics of percussive tools and their coupling to a human hand-arm system. This work is the first to leverage the COCO continuation framework to systematically detect and track grazing bifurcations in a nonsmooth hybrid model of a tool-hand interface.

To carry out this study, a lumped parameter model adapted from the work of Alabi *et al.* is employed to represent the percussive tool as a two-degree-of-freedom (2-DOF) vibro-impact system, while the hand-arm system is modeled as a separate 2-DOF lumped parameter system [26]. The resulting nonsmooth hybrid system is smoothened using Filippov's method, enabling both qualitative analysis via numerical bifurcation techniques and hy-

brid orbit continuation using the COCO toolbox.

The remainder of the paper is organized as follows. Section 1 presents the mathematical model of the vibro-impact HAS–HHIM system, outlines the smoothing procedure applied to the nonsmooth dynamics, and describes the continuation scheme used to track grazing orbits. Section 2 presents the major findings of the study, followed by a discussion of their implications in Section 3. Finally, conclusions are summarized in Section 3.

1 Model development of HHIM-HAS-NVAI system

In this section, we present the reduced-order vibro-impact model of the coupled HAS-HHIM system adapted from [26]. The schematic of the system is shown in Fig.1. In the schematic, the bit of the HHIM is modeled as a lumped mass, m_p, whereas the housing of the HHIM is modeled as a lumped mass m_H. The buffer between the HHIM bit and casing is modeled as a viscoelastic connection with parameters k_H and c_H. In this model, we also account for the feed force to press the machine against the material being worked on.

To capture the HHIM dynamics associated with the percussive action of the HHIM piston on the HHIM bit, a nonlinear interaction is specified between the HHIM bit and the ground material. To do so, the ground material is modeled as a linear spring–damper as presented in [25, 46, 47] with the initial separation of g from the HHIM bit. In this model, the ground material is restored before each successive impact, and the process of penetration of material is not taken into consideration. In this work, we consider concrete as the ground material with the stiffness and loss factors adopted from [46].

It is acknowledged that the present model may not capture all aspects of the physical dynamics due to the absence of advanced tool-tip representations such as viscoelastic connections with drift. Drift mechanisms can represent the net penetration of the tool bit into the material over time—an effect not accounted for in this formulation. Future studies could incorporate such features to examine whether the inclusion of drift provides additional insight beyond that offered by the simple viscoelastic contact model employed here.

Similarly, the hand-arm system is modeled as a 2-DOF lumped parameter system, which has been shown to provide an accurate representation of hand-transmitted vibrations at frequencies below 100 Hz [48]. As the operating frequency of the system in this study is approximately 45 Hz, the 2-DOF model is deemed sufficient for capturing the relevant dynamic response.

1.1 Non-smooth model

As similarly performed by Alabi *et al.* [26], the nonsmooth system is smoothened via the procedure below. In the schematic, x_H, x_a, x_p, and y represent the motion of the HHIM casing, HAS, HHIM bit, and massless support, respectively.

Due to the discontinuous nature of the HAS-HHIM system, the governing equations of motion are defined by two sets of differential equations: one for the contact phase and another for the non-contact phase. Defining f_m as the contact force between m_p and the material, the transition logic is given by:

$$\begin{cases} x_p < g, \quad f_m = 0 & : \text{without contact,} \\ x_p \geq g, \quad f_m = -\left(k_m y + c_m \dot{y}\right) < 0 & : \text{with contact.} \end{cases} \tag{1}$$

Following Leine [41], we assume that the support relaxes rapidly between contact events, and thus its free motion is neglected. The resulting governing equations of motion become:

$$\begin{aligned} (m_H + m_s)\ddot{x}_H &= \dot{x}_a c_s + x_a k_s + \dot{x}_p c_H + x_p k_H \\ &\quad - \dot{x}_H (c_H + c_s) - x_H (k_H + k_s) + F_{feed}, \end{aligned} \tag{2a}$$

$$m_a \ddot{x}_a = -\dot{x}_a (c_a + c_s) - x_a (k_a + k_s) + \dot{x}_H c_s + x_H k_s, \tag{2b}$$

$$m_p \ddot{x}_p = \begin{cases} -\dot{x}_p (c_H + c_m) - (x_p - g) k_m - x_p k_H \\ \qquad + \dot{x}_H c_H + x_H k_H + F_w, \quad \text{with contact,} \\ -\dot{x}_p c_H - x_p k_H + \dot{x}_H c_H + x_H k_H + F_w, \quad \text{without contact.} \end{cases} \tag{2c}$$

Here, F_{feed} is the operator-applied feed force and F_w is the piston-induced excitation, defined as:

$$F_w = F_{ref} \left(\frac{\omega}{\omega_{ref}} \right)^2 \sin(\omega t). \tag{3}$$

To simulate the nonsmooth dynamics, the system is convexified using Filippov's theory [49]. The state space is split into:

$$\begin{aligned} \mathscr{V}_- &= \{x \in \mathbb{R}^n \mid h(x) < 0\}, \\ \Sigma &= \{x \in \mathbb{R}^n \mid h(x) = 0\}, \\ \mathscr{V}_+ &= \{x \in \mathbb{R}^n \mid h(x) > 0\}. \end{aligned}$$

The resulting inclusion is:

$$\dot{x}(t) \in F(t,x) = \begin{cases} f_-, & x \in \mathscr{V}_-, \\ \overline{\text{co}}\{f_-, f_+\}, & x \in \Sigma, \\ f_+, & x \in \mathscr{V}_+, \end{cases} \tag{4}$$

where the convex combination is:

$$\overline{\text{co}}\left\{f_-, f_+\right\} = \{(1-q) f_- + q f_+, q \in [0,1]\}.$$

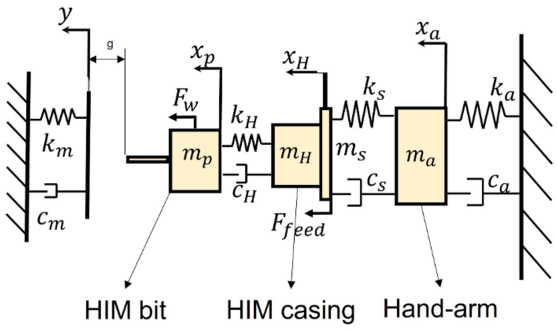

FIGURE 1: Schematic of the combined system of HHIM-HAS system

Switching boundaries are defined by:

$$h_\alpha(x_p, \dot{x}_p) = x_p - g, \tag{5}$$
$$h_\beta(x_p, \dot{x}_p) = k_m(x_p - g) + c_m \dot{x}_p. \tag{6}$$

The transitions are:

$$\mathscr{V}_- = \{x \mid h_\alpha < 0 \text{ or } h_\beta < 0\},$$
$$\mathscr{V}_+ = \{x \mid h_\alpha > 0 \text{ and } h_\beta > 0\},$$
$$\Sigma_\alpha = \{x \mid h_\alpha = 0, h_\beta \geq 0\},$$
$$\Sigma_\beta = \{x \mid h_\beta = 0, h_\alpha \geq 0\}.$$

1.2 Continuation segments for COCO

To facilitate the detection and tracking of grazing in the hybrid nonsmooth system using COCO, a periodic orbit is constructed by partitioning the trajectory into two segments, denoted by I_1 and I_2, each governed by a distinct vector field and transition logic. These segments represent two phases of the system's hybrid dynamics.

The angle variable θ is defined as $\theta = \omega t$, where ω is the angular frequency appearing in the excitation term:

$$F_w = F_{ref} \left(\frac{\omega}{\omega_{ref}} \right)^2 \sin(\omega t). \tag{7}$$

The transition between segments is implemented using COCO's multi-segment continuation structure. The following defines the event and reset functions used in each segment:

Segment I_1: No-contact dynamics with phase-based reset

$$\text{Event function:} \quad h_1(x) = \pi - \theta = \pi - \omega t,$$
$$\text{Reset map:} \quad x^+ = \left[x_H, \dot{x}_H, x_a, \dot{x}_a, x_p, \dot{x}_p, \theta - 2\pi\right]^\top.$$

This phase reset ensures continuity in the periodic orbit by wrapping the angular phase variable θ.

Segment I_2: No-contact dynamics with impact reset

$$\text{Event function:} \quad h_2(x) = x_p - g,$$
$$\text{Reset map:} \quad x^+ = x.$$

This reset corresponds to the event of bit contact with the ground. The reset is the identity map, as no discrete jump in the event of grazing.

For direct numerical integration, the differential equation is integrated using the smoothing switch model introduced by Leine [50], with smoothing thickness 2η applied around the switching surface. While for the continuation of the solutions of the system, the *hspo* toolbox COCO is used [51].

2 RESULTS

In this section, we begin by validating the chipping hammer model using its frequency response characteristics. Specifically, system parameters are tuned so that the model reproduces natural frequency peaks observed experimentally in the hand acceleration frequency response function (FRF). Following validation, we use bifurcation diagrams to identify the presence of grazing phenomena in the system. A two-parameter continuation study is then performed using COCO to examine how variations in operating parameters—namely the excitation amplitude F_{ref} and frequency ω—influence the onset of grazing. Finally, we conduct

TABLE 1: Parameter values of the HHIM-HAS-NLTVA system used for simulations.

Parameter	Value	Unit	Parameter	Value	Unit	Parameter	Value	Unit
m_H	8	kg	k_H	4×10^6	N/m	c_H	500	Ns/m
m_a	1.55	kg	k_a	4279	N/m	c_a	76	Ns/m
m_s	0.049	kg	k_s	62804	N/m	c_s	193	Ns/m
F_{ref}	80	N	ω_{ref}	30	Hz	g	0.02	m
m_p	0.35	kg	F_{feed}	40	N	k_m	3×10^6	N/m
c_m	50	Ns/m	–	–	–	–	–	–

a parametric study to investigate how changes in the tool's feed force affect the emergence and progression of grazing bifurcations. We also investigate the behavior of the hand-arm in different grazing regimes.

2.1 Validation of Chipping Hammer Dynamics

The validation of the chipping hammer model is done by tuning the system parameters so that the resulting hand-arm acceleration frequency response function (FRF), obtained via bifurcation diagrams, exhibits certain natural frequency peaks. These peaks are selected to match those observed experimentally in the FRF of a chipping hammer measured at the tool handle. Validation based on natural frequencies is essential, as it ensures the model accurately captures the frequencies at which vibration intensity at the hand is amplified. Experimental studies have shown that the hand acceleration FRF of a chipping hammer typically exhibits distinct peaks near the dominant operating frequency of the tool [52] and near the natural frequency of the chipping hammer handle [53]. Accordingly, the model parameters presented in Table 1 are selected so that the tool exhibits dominant frequency peaks near 45 Hz—corresponding to the tool's operating frequency—and around 600 Hz, which aligns with the resonance of the hammer handle. The resulting hand acceleration FRF, showing these characteristic peaks, is obtained using MATLAB's `ode45` solver with tight relative and absolute tolerances (10^{-11}) to integrate the system's first-order ODEs. The excitation frequency was swept across a defined range, and for each value, the system was numerically evolved to steady-state through repeated simulations. From the steady-state response, the *peak hand-arm acceleration* was extracted and plotted against frequency to capture the system's resonance behavior and validate the dynamic model as shown in Fig. 2.

2.2 Grazing Detection and Orbit Initialization for Continuation

Having selected the system parameters, the excitation amplitude of the chipping hammer is varied to generate a frequency response function (FRF) that exhibits grazing behavior. This FRF is constructed by plotting the amplitude of the tool tip in order to identify the points where the tool tip grazes the ground, defined at $x_p = g = 0.02\,\text{m}$. As shown in Fig. 3a, the system exhibits grazing at two distinct points, labeled G_1 and G_2.

To investigate how the system's grazing behavior evolves, we construct an initial solution guess in the form of a periodic orbit corresponding to the grazing point G_2. The resulting orbit is shown in the phase portrait in Fig. 3b. This trajectory consists of two segments, $\mathscr{I}_1$ and $\mathscr{I}_2$, corresponding to distinct phases of the hybrid system dynamics, as previously described. The orbit is obtained via direct numerical integration of the smooth vector fields, with event and reset conditions applied at each segment boundary. This trajectory serves as the initial guess for hybrid orbit continuation in COCO.

To enable grazing continuation, a grazing event constraint is appended to the problem. Specifically, grazing is detected when the tool tip reaches the ground with zero normal velocity. This is enforced by monitoring the impact condition $h(x) = x_p - g = 0$ along with the tangency condition $\dot{x}_p = 0$ at the point of contact. A pairwise parameter continuation is then carried out, allowing the chipping hammer's operating parameters to vary while constraining the orbit to remain at the grazing condition.

The resulting continuation curve in the chipping hammer's operating parameter space (ω, F_{ref}) is shown in Fig. 4. The continuation begins at the grazing point labeled G_1 and identifies a second grazing point G_2, as previously shown in Fig. 3a. The study reveals that for lower values of F_{ref}, the system does not exhibit grazing (labeled region A in the diagram). However, at higher values of F_{ref}, two distinct grazing points emerge (labeled region B). As the excitation amplitude is further increased, one of these grazing points disappears, indicating a boundary in the grazing region (labeled region C). To explore how the system

dynamics vary with model parameters, we perform a parametric study by varying the feed force (F_{feed}). This enables us to evaluate the resulting changes in the grazing curve within the (ω, F_{ref}) space, as well as the corresponding effect on the hand-arm system response.

2.3 Effect of Feed Force on Grazing Behavior

From Fig. 4b, we observe that an increase in F_{feed} leads to a decrease in the excitation amplitude at which grazing first occurs in the system; that is, Region A in Fig. 4a becomes wider. The study also reveals that with increasing feed force, the range of frequency values ω at which grazing occurs becomes more spread out. This behavior can be observed by comparing the grazing curves for $F_{\text{feed}} = 20$ N and $F_{\text{feed}} = 40$ N at $F_{\text{ref}} = 85$ N, where the lower and upper bounds of grazing shift apart — the lower grazing frequency decreases while the upper one increases as feed force increases. In addition to this widening of the grazing frequency interval, we also observe a transition in the number of grazing points. At $F_{\text{ref}} = 80$ N for $F_{\text{feed}} = 40$ N, grazing occurs at two distinct frequencies, whereas at $F_{\text{feed}} = 60$ N , only one grazing point is observed.

Based on these observations, it can be concluded that feed force affects both the onset and nature of grazing in the system. Variations in feed force shift the excitation amplitude at which grazing begins and alter the frequency values at which grazing occurs for a given excitation amplitude level. Additionally, feed force influences the number of grazing points observed. In some cases, the system transitions from exhibiting two grazing points to just one as feed force increases.

2.4 Effect of grazing regimes on hand-arm acceleration Frequency Response

To assess how different grazing regimes influence vibrations at the hand-arm interface, we present acceleration frequency response functions (FRFs) at the hand. As shown in Fig. 5, three FRFs are obtained by keeping the feed force constant while varying the excitation force amplitude F_{ref} to position the system in grazing regimes A, B, and C, as defined in Fig. 4.

Initial observations indicate that as the excitation amplitude increases—from Region A (no grazing) to Region C (single grazing)—the overall amplitude of the hand-arm acceleration increases accordingly. A closer examination of Fig. 5 reveals that at both $\omega = 550$ Hz and the system's operating frequency of 45 Hz, a transition from Region A to B results in a 150% increase in acceleration at the hand, while the transition from Region B to C yields a 20% increase. However, the presence or absence of grazing does not appear to significantly affect the damping ratio or shift the natural frequencies observed in the FRF.

Although the current study, as shown through the FRF in Fig. 5, does not explicitly observe bifurcations or chaotic dynamics within Regions B or C with the onset of grazing, it is important to recognize that grazing events often act as precursors to qualitative transitions in nonsmooth systems. Specifically, grazing can lead to the onset of chaotic motion, multistability, or the sudden disappearance of stable periodic orbits [28, 35]. Region B, characterized by two grazing events per cycle, may be particularly susceptible to such transitions under perturbations in the system's parameters. Region C, with a single grazing point, similarly represents a regime near the boundary of qualitative change. While a detailed investigation of these behaviors lies beyond the scope of the present work, future studies could employ tools such as Lyapunov exponent analysis or Poincaré mapping to explore the potential for quasiperiodic or chaotic dynamics in these regimes. Such behaviors, if present, may also correlate with increased variability or amplification in the acceleration transmitted to the hand, further emphasizing the need to characterize grazing-induced transitions.

These results suggest that the observed rise in hand-arm acceleration is likely driven primarily by the increase in excitation force, rather than by grazing phenomena themselves. This raises an important question: does grazing meaningfully influence the hand-arm response, or is its effect negligible compared to excitation amplitude? A more detailed investigation may be required to isolate the role of grazing and determine whether it contributes independently to the vibration intensity perceived at the hand.

3 DISCUSSION

The results of the parametric study suggest that the onset of grazing in the tool is significantly influenced by the level of feed force applied. Specifically, the findings show that increasing or decreasing the applied feed force can either eliminate or induce grazing behavior within the system. This sensitivity of grazing to feed force reinforces prior experimental observations that feed force plays a critical role in determining the acceleration output at the handle [52].

However, analysis of the hand-arm acceleration across different grazing regimes—including regions of no grazing, single grazing, and dual grazing—revealed that the presence or absence of grazing does not substantially alter the shape or structure of the hand-arm acceleration FRF. Instead, increases in acceleration amplitude appear to be primarily driven by changes in excitation force. This finding challenges the original hypothesis that grazing significantly affects the vibrations transmitted to the hand.

These observations highlight the need for experimental validation to determine whether the emergence or disappearance of grazing meaningfully influences hand-arm acceleration in practice. They also motivate further refinement of the vibroimpact model to enhance its predictive fidelity for vibration transmission to the user. In particular, improving how the model captures contact dynamics and coupling with the hand-arm system could offer better alignment between simulated and experimentally observed behavior.

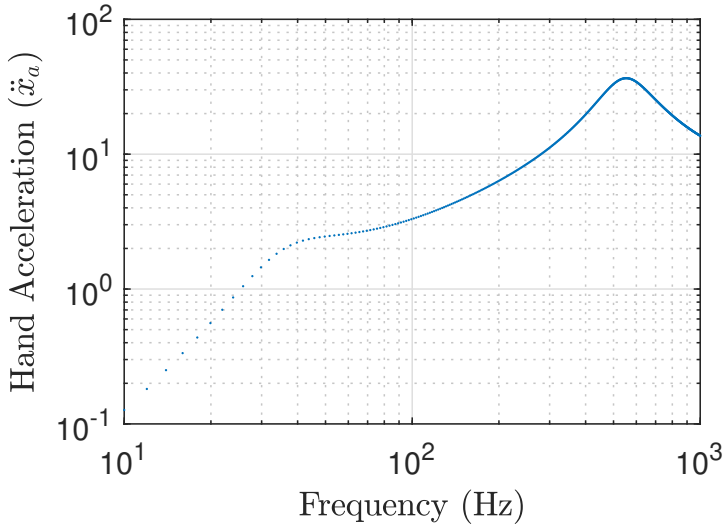

(a)

FIGURE 2: Frequency response function (FRF) of hand acceleration $\ddot{x}_a$ versus excitation frequency, showing resonance peaks at approximately 45 Hz and 600 Hz. These peaks correspond to the natural frequencies of the modeled system and reflect trends typical of the chipping hammer handle experimental vibration data.

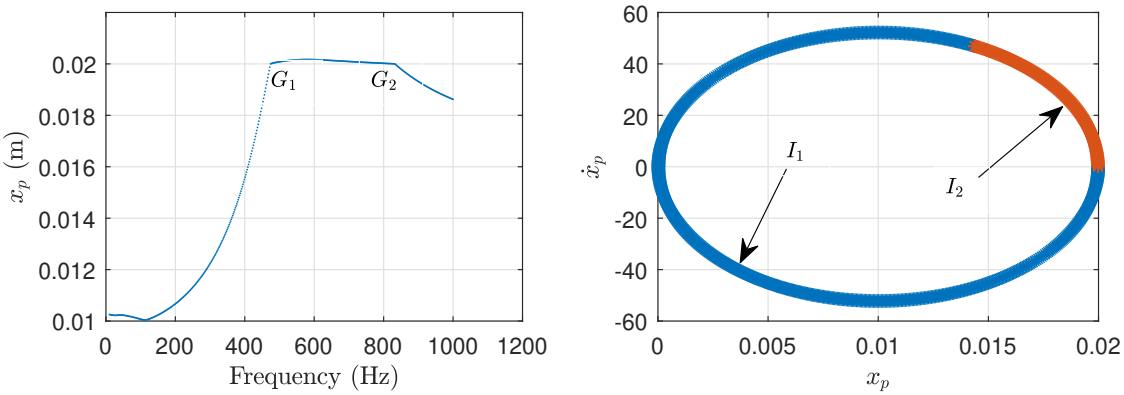

(a) (b)

FIGURE 3: a) Bifurcation diagram showing two points where the system grazes as reflected by the tooltip displacement at xp =0.02. b) The phase portrait which is used as the initial multisegment solution to be fed into COCO's hspo toolbox. Both diagrams are generated using the parameters in Table 1.

Conclusion

This study explored the nonlinear dynamics of a chipping hammer system to better understand how grazing behavior influences vibrations transmitted to the hand-arm interface. A vibroimpact model was developed to represent the percussive nature of the tool and was coupled to a hand-arm system. The model parameters were tuned to match experimentally observed natural frequencies of a chipping hammer.

Using numerical continuation via the COCO toolbox, grazing bifurcations were systematically identified in the (ω, F_{ref}) parametric space. The results revealed that grazing events appear and disappear based on changes in excitation amplitude. At low excitation levels, the system exhibits no grazing; at higher amplitudes, two grazing points emerge, which eventually merge into a single grazing point as excitation increases further.

A parametric study was conducted to examine how varying

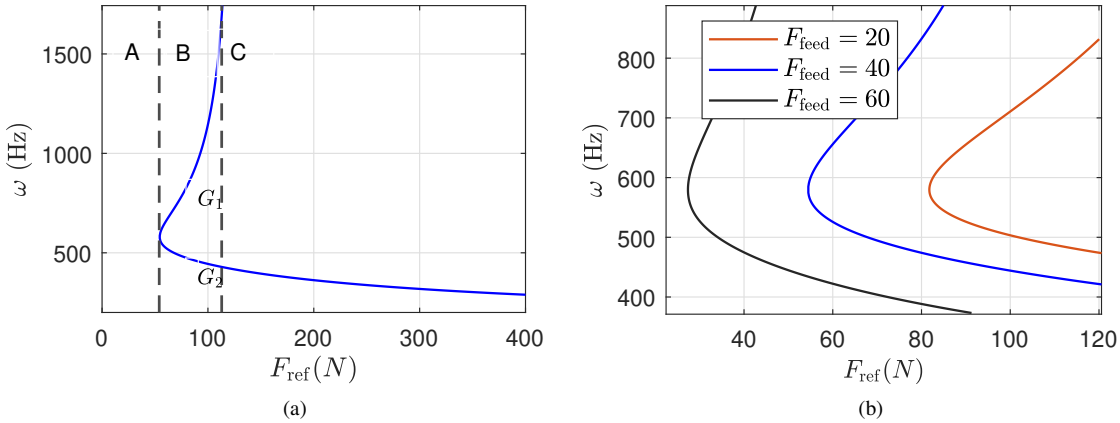

(a) (b)

FIGURE 4: a) Continuation of grazing points in the (ω, F_{ref}) parametric space. The previously identified grazing points G_1 and G_2 from Fig. 3a are marked along the grazing curve. Region A corresponds to parameter values where no grazing occurs, Region B indicates the presence of two distinct grazing points, and Region C marks the boundary beyond which one grazing point disappears. b) Comparison of grazing curves in the (ω, F_{ref}) space for three different feed force values.

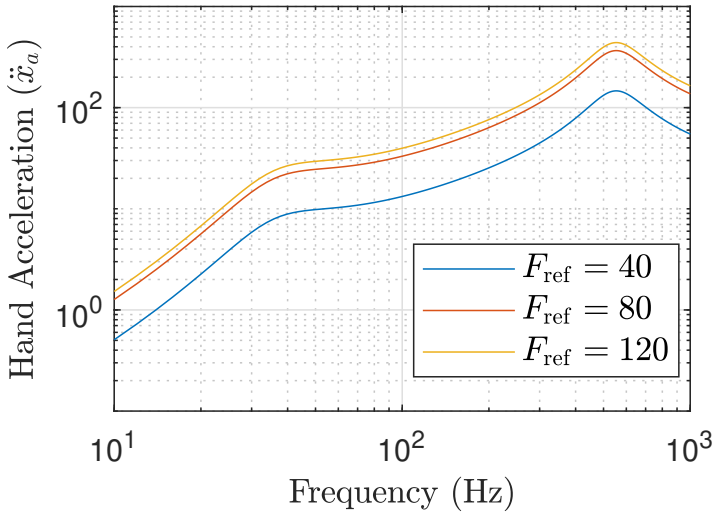

(a)

FIGURE 5: Comparison of hand-arm acceleration across different grazing regimes for $F_{feed} = 40N$. At $F_{\text{ref}} = 40$ N, the system operates in Region A where no grazing occurs, as seen in Fig. 4. At $F_{\text{ref}} = 100$ N, the system grazes at two frequencies (Region B), while at $F_{\text{ref}} = 120$ N, grazing occurs at only one frequency (Region C). This figure highlights how transitions between grazing regimes influence the vibration response at the hand-arm interface.

the feed force affects grazing behavior. The results show that increasing the feed force lowers the excitation amplitude at which grazing begins and broadens the frequency interval over which grazing occurs. In some cases, feed force was also found to change the number of grazing points from two to one, indicating a shift in the underlying system dynamics. However, despite these shifts in grazing characteristics, their effect on hand-arm acceleration was relatively modest.

These findings suggest that while feed force is a useful parameter for modulating the onset and structure of grazing in the system, the resulting changes in vibration at the hand may not be strongly tied to grazing behavior alone. This highlights the need

for further experimental validation and points to the potential for improving the vibroimpact model to more accurately capture the complex interaction between tool dynamics and hand-arm response.

REFERENCES

[1] Harada, N., and Mahbub, M., 2008. "Diagnosis of vascular injuries caused by hand-transmitted vibration". *International archives of occupational and environmental health,* ***81***(5), pp. 507–518.

[2] De Silva, G. S., and Wijewardana, T., 2021. "Preliminary results of hand arm vibration (hav) exposures of chipping hammer operators in tropical weather: Analysis of exposures and protective gloves". *International Journal of Industrial Ergonomics,* ***86***, p. 103197.

[3] Griffin, M. J., 2012. *Handbook of human vibration*. Academic press.

[4] Bernard, B. P., and Putz-Anderson, V., 1997. "Musculoskeletal disorders and workplace factors; a critical review of epidemiologic evidence for work-related musculoskeletal disorders of the neck, upper extremity, and low back".

[5] ISO, I., 2001. "5349-1: Mechanical vibration—measurement and evaluation of human exposure to hand-transmitted vibration—part 1: general requirements". *Geneva, Switzerland: International Organization for Standardization*.

[6] Vihlborg, P., Bryngelsson, L., Lindgren, B., Gunnarsson, L. G., and Graff, P., 2017. "Association between vibration exposure and hand-arm vibration symptoms in a swedish mechanical industry". *International Journal of Industrial Ergonomics,* ***62***, pp. 77–81.

[7] Griffin, M., Bovenzi, M., and Nelson, C., 2003. "Dose-response patterns for vibration-induced white finger". *Occupational and Environmental Medicine,* ***60***(1), pp. 16–26.

[8] Dong, R. G., Wu, J. Z., and Welcome, D. E., 2005. "Recent advances in biodynamics of human hand-arm system". *Industrial health,* ***43***(3), pp. 449–471.

[9] Barregard, L., Ehrenström, L., and Marcus, K., 2003. "Hand-arm vibration syndrome in swedish car mechanics". *Occupational and environmental medicine,* ***60***(4), pp. 287–294.

[10] Institute, A. N. S., 1986. *Guide for the Measurement and Evaluation of Human Exposure to Vibration Transmitted to the Hand*.

[11] Moschioni, G., Saggin, B., and Tarabini, M., 2011. "Prediction of data variability in hand-arm vibration measurements". *Measurement,* ***44***(9), pp. 1679–1690.

[12] Saggin, B., Scaccabarozzi, D., and Tarabini, M., 2012. "Optimized design of suspension systems for hand–arm transmitted vibration reduction". *Journal of sound and vibration,* ***331***(11), pp. 2671–2684.

[13] Jahn, R., and Hesse, M., 1986. "Applications of hand-arm models in the investigation of the interaction between man and machine". *Scandinavian journal of work, environment & health*, pp. 343–346.

[14] Śledziński, M., 2014. "Proposed model of hand for designing ergonomic vibration isolation systems for hand-held impact tools". *American Journal of Mechanical Engineering,* ***2***(7), pp. 290–294.

[15] Aguiar, R., d'Almeida, E., and Ritto, T., 2020. "Vibro-impact model and validation of the axial dynamics of a vibration-assisted drilling tool". *Journal of the Brazilian Society of Mechanical Sciences and Engineering,* ***42***, pp. 1–16.

[16] Pavlovskaia, E., Hendry, D. C., and Wiercigroch, M., 2015. "Modelling of high frequency vibro-impact drilling". *International Journal of Mechanical Sciences,* ***91***, pp. 110–119.

[17] Pavlovskaia, E., Wiercigroch, M., and Grebogi, C., 2001. "Modeling of an impact system with a drift". *Physical Review E,* ***64***(5), p. 056224.

[18] Alabi, O., Gupta, S. K., and Barry, O., 2023. "Vibration analysis of a nonlinear absorber coupled to a hand-held impact machine". *Journal of Computational and Nonlinear Dynamics*, pp. 1–18.

[19] Wiercigroch, M., and Pavlovskaia, E., 2003. "Nonlinear dynamics of vibro-impact systems: theory and experiments". In Materials science forum, Vol. 440, Trans Tech Publ, pp. 513–520.

[20] Cao, Q.-J., Wiercigroch, M., Pavlovskaia, E., and Yang, S.-P., 2010. "Bifurcations and the penetrating rate analysis of a model for percussive drilling". *Acta Mechanica Sinica,* ***26***(3), pp. 467–475.

[21] Wiercigroch, M., 2006. "Applied nonlinear dynamics of non-smooth mechanical systems". *Journal of the Brazilian Society of Mechanical Sciences and Engineering,* ***28***(4), pp. 519–526.

[22] Ho, J.-H., Nguyen, V.-D., and Woo, K.-C., 2011. "Nonlinear dynamics of a new electro-vibro-impact system". *Nonlinear dynamics,* ***63***(1), pp. 35–49.

[23] Adly, S., and Goeleven, D., 2020. "A nonsmooth approach for the modelling of a mechanical rotary drilling system with friction". *Evolution Equations and Control Theory,* ***10***.

[24] Liao, M., Liu, Y., Chávez, J. P., Chong, A. S., and Wiercigroch, M., 2018. "Dynamics of vibro-impact drilling with linear and nonlinear rock models". *International Journal of Mechanical Sciences,* ***146***, pp. 200–210.

[25] Wiercigroch, M., Wojewoda, J., and Krivtsov, A., 2005. "Dynamics of ultrasonic percussive drilling of hard rocks". *Journal of Sound and Vibration,* ***280***(3-5), pp. 739–757.

[26] Alabi, O., Gupta, S., and Barry, O. R., 2024. "Hand vibration reduction using nonlinear vibration absorber for the vibro-impact hammer model". *Journal of Computational*

and Nonlinear Dynamics, ***19***(7).

[27] Banerjee, B., Bajaj, A. K., and Davies, P., 1996. "Resonant dynamics of an autoparametric system: a study using higher-order averaging". *International Journal of Non-Linear Mechanics,* ***31***(1), pp. 21–39.

[28] Bernardo, M., Budd, C., Champneys, A. R., and Kowalczyk, P., 2008. *Piecewise-smooth dynamical systems: theory and applications*, Vol. 163. Springer Science & Business Media.

[29] Ganguli, A., and Banerjee, S., 2005. "Dangerous bifurcation at border collision: When does it occur?". *Physical Review E—Statistical, Nonlinear, and Soft Matter Physics,* ***71***(5), p. 057202.

[30] Ma, Y., Agarwal, M., and Banerjee, S., 2006. "Border collision bifurcations in a soft impact system". *Physics Letters A,* ***354***(4), pp. 281–287.

[31] Chávez, J. P., Brzeski, P., and Perlikowski, P., 2017. "Bifurcation analysis of non-linear oscillators interacting via soft impacts". *International Journal of Non-Linear Mechanics,* ***92***, pp. 76–83.

[32] Yin, S., Ji, J., and Wen, G., 2019. "Complex near-grazing dynamics in impact oscillators". *International Journal of Mechanical Sciences,* ***156***, pp. 106–122.

[33] Yin, S., Ji, J., Deng, S., and Wen, G., 2019. "Degenerate grazing bifurcations in a three-degree-of-freedom impact oscillator". *Nonlinear Dynamics,* ***97***, pp. 525–539.

[34] Yin, S., Wen, G., Ji, J., and Xu, H., 2020. "Novel two-parameter dynamics of impact oscillators near degenerate grazing points". *International Journal of Non-Linear Mechanics,* ***120***, p. 103403.

[35] Nordmark, A. B., 1991. "Non-periodic motion caused by grazing incidence in an impact oscillator". *Journal of Sound and Vibration,* ***145***(2), pp. 279–297.

[36] Dankowicz, H., and Paul, M. R., 2009. "Discontinuity-induced bifurcations in systems with hysteretic force interactions".

[37] Hu, S., and Raman, A., 2006. "Chaos in atomic force microscopy". *Physical Review Letters,* ***96***(3), p. 036107.

[38] Shaw, S. W., and Holmes, P., 1983. "Periodically forced linear oscillator with impacts: chaos and long-period motions". *Physical Review Letters,* ***51***(8), p. 623.

[39] Vasconcellos, R., Abdelkefi, A., Hajj, M. R., and Marques, F. D., 2014. "Grazing bifurcation in aeroelastic systems with freeplay nonlinearity". *Communications in Nonlinear Science and Numerical Simulation,* ***19***(5), pp. 1611–1625.

[40] Wiercigroch, M., 2000. "Modelling of dynamical systems with motion dependent discontinuities". *Chaos, Solitons & Fractals,* ***11***(15), pp. 2429–2442.

[41] Leine, R. I., 2000. "Bifurcations in discontinuous mechanical systems of the fillippov-type".

[42] Savi, M. A., Divenyi, S., Franca, L. F. P., and Weber, H. I., 2007. "Numerical and experimental investigations of the nonlinear dynamics and chaos in non-smooth systems". *Journal of Sound and Vibration,* ***301***(1-2), pp. 59–73.

[43] Wolf, H., Kodvanj, J., and Bjelovučić-Kopilović, S., 2004. "Effect of smoothing piecewise-linear oscillators on their stability predictions". *Journal of sound and vibration,* ***270***(4-5), pp. 917–932.

[44] Zhang, Z., Páez Chávez, J., Sieber, J., and Liu, Y., 2022. "Controlling grazing-induced multistability in a piecewise-smooth impacting system via the time-delayed feedback control". *Nonlinear Dynamics,* ***107***(2), pp. 1595–1610.

[45] Chávez, J. P., Zhang, Z., and Liu, Y., 2020. "A numerical approach for the bifurcation analysis of nonsmooth delay equations". *Communications in Nonlinear Science and Numerical Simulation,* ***83***, p. 105095.

[46] Golysheva, E., Babitsky, V., and Veprik, A., 2004. "Vibration protection for an operator of a hand-held percussion machine". *Journal of Sound and Vibration,* ***274***(1-2), pp. 351–367.

[47] Wiercigroch, M., Neilson, R., and Player, M., 1999. "Material removal rate prediction for ultrasonic drilling of hard materials using an impact oscillator approach". *Physics Letters A,* ***259***(2), pp. 91–96.

[48] Dong, R. G., Welcome, D. E., Wu, J. Z., and McDowell, T. W., 2008. "Development of hand-arm system models for vibrating tool analysis and test rig construction". *Noise Control Engineering Journal,* ***56***(1), pp. 35–44.

[49] Filippov, A. F., 2013. *Differential equations with discontinuous righthand sides: control systems*, Vol. 18. Springer Science & Business Media.

[50] Leine, R. I., and Nijmeijer, H., 2013. *Dynamics and bifurcations of non-smooth mechanical systems*, Vol. 18. Springer Science & Business Media.

[51] Dankowicz, H., and Schilder, F., 2013. *Recipes for continuation*. SIAM.

[52] Dong, R., McDowell, T., Welcome, D., Warren, C., and Schopper, A., 2004. "An evaluation of the standardized chipping hammer test specified in iso 8662-2". *Annals of occupational hygiene,* ***48***(1), pp. 39–49.

[53] Monazzam, M. R., Khavanin, A., Sarrafzadeh, O., Parsaeian, M., and Azrah, K., 2023. "Handle transmitted vibration of electrical demolition hammers: Frequency and magnitude investigation in field measurements from different bits". *Journal of Low Frequency Noise, Vibration and Active Control,* ***42***(4), pp. 1880–1899.